

The Electronic Spectrum of  $\text{Re}_2\text{Cl}_8^{2-}$ : A Theoretical StudyLaura Gagliardi\*<sup>†</sup> and Björn O. Roos<sup>‡</sup>

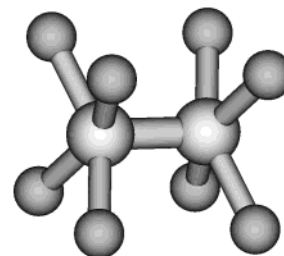
Dipartimento di Chimica Fisica F. Accascina, Viale delle Scienze—Parco d'Orleans II, I-90128 Palermo, Italy, and Department of Theoretical Chemistry, Chemical Center, P.O. Box 124, S-221 00 Lund, Sweden

Received October 14, 2002

One of the prototype compounds for metal–metal multiple bonding, the  $\text{Re}_2\text{Cl}_8^{2-}$  ion, has been studied theoretically using multiconfigurational quantum chemical methods. The molecular structure of the ground state has been determined. It is shown that the effective bond order of the Re–Re bond is close to three, due to the weakness of, in particular, the  $\delta$  bond. The electronic spectrum has been calculated with the inclusion of spin–orbit coupling. Observed spectral features have been reproduced with good accuracy, and a number of new assignments are suggested.

## 1. Introduction

In 1965, F. A. Cotton and C. B. Harris reported the crystal structure of  $\text{K}_2[\text{Re}_2\text{Cl}_8]\cdot 2\text{H}_2\text{O}$ .<sup>1</sup> A surprisingly short Re–Re distance of 2.24 Å was found. This was the first example of a multiple bond between two metal atoms, and the  $\text{Re}_2\text{Cl}_8^{2-}$  ion has since then become the prototype for this type of complexes. A new era of inorganic chemistry was born. Cotton analyzed the bonding using simple molecular orbital (MO) theory and concluded that a quadruple Re–Re bond was formed.<sup>1,2</sup> Two parallel  $\text{ReCl}_4$  units are connected by the Re–Re bond. The  $d_{x^2-y^2}$ ,  $p_x$ ,  $p_y$ , and  $s$  orbitals of the valence shell of each Re atom form the  $\sigma$  bonding to each Cl atom. The remaining  $d_z^2$  and  $p_z$  orbitals with  $\sigma$  symmetry relative to the Re–Re line, the  $d_{xz}$  and  $d_{yz}$  with  $\pi$  symmetry, and the  $d_{xy}$  with  $\delta$  symmetry form the quadruple Re–Re bond: one  $\sigma$  bond, two  $\pi$  bonds, and one  $\delta$  bond. Because there are eight electrons to occupy these MOs, the ground state configuration will be  $\sigma^2\pi^4\delta^2$ . The presence of the  $\delta$  bond explains the eclipsed conformation of the ion. In a staggered conformation, the overlap of the  $\delta$  atomic orbitals is zero, and the  $\delta$  bond disappears. The visible spectrum was also reported in these early studies. The notion of a quadruple bond is based on the inherent assumption that four bonding orbitals are doubly occupied. Today we know that this is not the case for weak intermetallic bonds. The true bond

**Figure 1.** Structure of  $\text{Re}_2\text{Cl}_8^{2-}$ .

order depends on the relation between the occupation of the bonding and antibonding orbitals, respectively. Such a description is, however, only possible if a quantum chemical model is used that goes beyond the Hartree–Fock model. Such a model will be used here, and we shall demonstrate that the true bond order between the two Re atoms is closer to three than to four.

Considering its fundamental character, the quadruple Re–Re bond in the dirhenium complex  $\text{Re}_2\text{Cl}_8^{2-}$  (Figure 1) has been a subject of several later studies both experimentally and theoretically.

In 1977 and 1978, Trogler et al.<sup>3,4</sup> measured the single-crystal polarized electronic absorption spectrum of  $\text{Re}_2\text{Cl}_8^{2-}$ , and they assigned various bands.

More recently, Blaudeau et al.<sup>5</sup> have studied  $\text{Re}_2\text{Cl}_8^{2-}$  by ab initio quantum chemical methods, following previous

\* To whom correspondence should be addressed. E-mail: laurag@ciam.unibo.it.

<sup>†</sup> Viale delle Scienze.

<sup>‡</sup> Chemical Center.

(1) Cotton, F. A.; Harris, C. B. *Inorg. Chem.* **1965**, *4*, 330.

(2) Cotton, F. A. *Inorg. Chem.* **1965**, *4*, 334.

(3) Trogler, W. C.; Cowman, C. D.; Gray, H. B.; Cotton, F. A. *J. Am. Chem. Soc.* **1977**, *99*, 2993.

(4) Trogler, W. C.; Gray, H. B. *Acc. Chem. Res.* **1978**, *11*, 232.

(5) Blaudeau, J.-P.; Ross, R. B.; Pitzer, R. M.; Mougnot, P.; Bénard, M. *J. Phys. Chem.* **1994**, *98*, 7123.

theoretical work by Hay.<sup>6</sup> They performed multiconfigurational self-consistent field (MCSCF) and configuration interaction (CI) calculations with relativistic effective core potentials at the experimental geometry of the complex.<sup>1,7</sup> The ground state and the two lowest excited states were studied.

However, none of these earlier studies gave a more complete treatment of the low-lying excited states, and the computed energies were not accurate enough to give an unambiguous assignment of the experimental spectrum. Today more advanced methods are available for such studies, which also include relativistic effects and spin-orbit coupling. Therefore, it should be possible to give a rather complete account of the electronic spectrum. Because the  $\text{Re}_2\text{Cl}_8^{2-}$  ion is such an important entity in inorganic chemistry, we decided to study its structure and electronic spectrum using multiconfigurational quantum chemistry, the only approach that can deal with the complexity of the multiple bond. The same approach used in the present work has earlier been used to describe successfully the properties and electronic spectrum of the  $\text{Cr}_2$  molecule, which formally has a sextuple bond,<sup>8,9</sup> and dichromium tetraformate.<sup>10</sup> The main difference here is that we include relativistic effects in a more adequate way, and also spin-orbit coupling.

## 2. Details of the Calculations

The study was performed using the complete active space (CAS) SCF method<sup>11</sup> with dynamic correlation added by multiconfigurational second-order perturbation theory (CASPT2).<sup>12–14</sup> Scalar relativistic effects were included via a Douglas–Kroll (DK) Hamiltonian.<sup>15,16</sup> The effects of spin-orbit (SO) coupling were calculated employing a newly developed method based on the CASSCF state interaction method (CASSI).<sup>17,18</sup> Here, the CASSCF wave functions generated for a number of electronic states are allowed to mix under the influence of a spin-orbit Hamiltonian. The method has recently been described, and we refer to this article for details.<sup>19</sup> It has been shown to be successful in the study of actinide compounds.<sup>20,21</sup> All calculations have been performed with the software MOLCAS-5.<sup>22</sup>

A newly developed basis set of ANO type has been used for Re and Cl atoms.<sup>23</sup> They are of the atomic natural orbital (ANO) type

with the expansion coefficients optimized in CASSCF/CASPT2 calculations on different spectroscopic states of the atom and positive ion (for Cl on the negative ion). The DK Hamiltonian was used to include scalar relativistic effects. We note that such a basis set can only be used in relativistic calculations. For Re, the primitive set 24s20p15d11f3g was contracted to 8s7p5d3f in a first set of calculations (basis set B1) and also to 8s7p5d3f1g (basis set B2). For Cl, the primitive set 17s12p5d3f was contracted to 5s4p2d (B1) and to 5s4p2d1f (B2).

The geometry of the ground state was optimized at the CASSCF level using analytical first derivatives<sup>24</sup> and assuming that the molecule has  $D_{2h}$  symmetry. Since MOLCAS works in subgroups of  $D_{2h}$ , all calculations were performed in  $D_{2h}$  symmetry. A numerical optimization of the three degrees of freedom of the molecule, the Re–Re and Re–Cl bonds and ClReRe angle, was also carried out at the CASPT2 level.

The choice of the active space is the crucial step in a CASSCF/CASPT2 calculation. Initially, an active space formed by 12 electrons in 12 active orbitals (12/12) was used. This comprises one 5d $\sigma$ , two 5d $\pi$ , and one 5d $\delta$  Re–Re bonding orbitals and the corresponding antibonding orbitals and two Re–Cl  $\delta$  bonding orbitals and the corresponding two antibonding MOs. This active space can only describe electronic states where the excitations are located in the Re–Re bond. An extension is needed to cover also the ligand-to-metal charge-transfer (LMCT) excitations. It would be impossible to include all the Cl 3p orbitals in the active space. Therefore, a more limited procedure was followed: The active space was enlarged with two orbitals in one of the eight irreps of  $D_{2h}$  and four extra electrons. Thus, eight sets of calculations were performed with a 16/14 active space. Calculations were only performed for allowed transitions (symmetries  ${}^1A_{2u}$  and  ${}^1E_u$ ). This procedure will have the effect that a number of excited states are computed with different active spaces, which can be used to check whether the results are stable when the active space is enlarged.

## 3. Results

**3.1. The Ground State.** The geometry of  $\text{Re}_2\text{Cl}_8^{2-}$  obtained at the CASSCF and CASPT2 levels of theory with two different basis sets is reported in Table 1, together with the experimental values.

The small basis, B1, reproduces reasonably well the Re–Re distance, while it gives a too long Re–Cl distance. The CASSCF and CASPT2 results obtained with the B1 basis set are very similar. With the large basis, on the other hand, the Re–Cl distance improves substantially in going from CASSCF to CASPT2. It thus seems that the inclusion of

- (6) Hay, P. J. *J. Am. Chem. Soc.* **1982**, *104*, 7007.
- (7) Chakravarty, A. R.; Cotton, F. A.; Cutler, A. R.; Walton, R. A. *Inorg. Chem.* **1986**, *25*, 3619.
- (8) Andersson, K. *Chem. Phys. Lett.* **1995**, *237*, 212.
- (9) Roos, B. O.; Andersson, K. *Chem. Phys. Lett.* **1995**, *245*, 215.
- (10) Andersson, K.; Bauschlicher, C. W., Jr.; Persson, B. J.; Roos, B. O. *Chem. Phys. Lett.* **1996**, *257*, 238.
- (11) Roos, B. O. In *Advances in Chemical Physics; Ab Initio Methods in Quantum Chemistry-II*; Lawley, K. P., Ed.; John Wiley & Sons Ltd.: Chichester, U.K., 1987; p 399.
- (12) Andersson, K.; Malmqvist, P.-Å.; Roos, B. O.; Sadlej, A. J.; Wolinski, K. *J. Phys. Chem.* **1990**, *94*, 5483.
- (13) Andersson, K.; Malmqvist, P.-Å.; Roos, B. O. *J. Chem. Phys.* **1992**, *96*, 1218.
- (14) Roos, B. O.; Andersson, K.; Fülcher, M. P.; Malmqvist, P.-Å.; Serrano-Andrés, L.; Pierloot, K.; Merchán, M. In *Advances in Chemical Physics: New Methods in Computational Quantum Mechanics, Vol. XCIII*; Prigogine, I., Rice, S. A., Eds.; John Wiley & Sons: New York, 1996; pp 219–331.
- (15) Douglas, N.; Kroll, N. M. *Ann. Phys.* **1974**, *82*, 89.
- (16) Hess, B. *Phys. Rev. A* **1986**, *33*, 3742.
- (17) Malmqvist, P.-Å. *Int. J. Quantum Chem.* **1986**, *30*, 479.
- (18) Malmqvist, P.-Å.; Roos, B. O. *Chem. Phys. Lett.* **1989**, *155*, 189.
- (19) Malmqvist, P.-Å.; Roos, B. O.; Schimmelpfennig, B. *Chem. Phys. Lett.* **2002**, *357*, 230.

- (20) Gagliardi, L.; Roos, B. O.; Malmqvist, P.-Å.; Dyke, J. M. *J. Phys. Chem. A* **2001**, *105*, 10602.
- (21) Roos, B. O.; Malmqvist, P.-Å.; Gagliardi, L. *Heavy element quantum chemistry - the multiconfigurational approach*; Brändas, E. J., Kryachko, E. S., Eds.; Fundamental World of Quantum Chemistry: A Tribute Volume to the Memory of Per-Olov Löwdin; Kluwer: Dordrecht, The Netherlands, 2003; Vol. 2, Chapter 16.
- (22) Andersson, K.; Baryz, M.; Bernhardsson, A.; Blomberg, M. R. A.; Carissan, Y.; Cooper, D. L.; Cossi, M.; Fleig, T.; Flscher, M. P.; Gagliardi, L.; de Graaf, C.; Hess, B. A.; Karlström, G.; Lindh, R.; Malmqvist, P.-Å.; Neogrady, P.; Olsen, J.; Roos, B. O.; Schimmelpfennig, B.; Schtz, M.; Seijo, L.; Serrano-Andrés, L.; Siegbahn, P. E. M.; Strling, J.; Thorsteinsson, T.; Veryazov, V.; Wierzbowska, M.; Widmark, P.-O. *MOLCAS Version 5.2*; Department of Theoretical Chemistry, Chemical Center, University of Lund: Lund, Sweden, 2001.
- (23) Roos, B. O.; Widmark, P.-O. *Theor. Chem. Acc.*, submitted.
- (24) Lindh, R. *Theor. Chim. Acta* **1993**, *85*, 423.

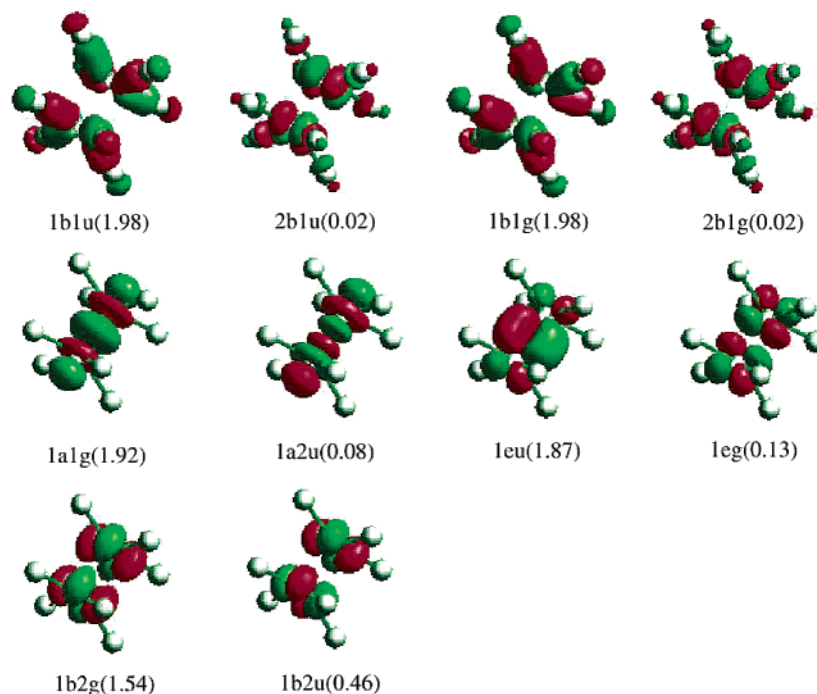


**Figure 2.** Natural orbitals in the  $[\text{Re}_2\text{Cl}_8]^{2-}$  ion. The label and occupation number is given for each orbital.

**Table 1.** Structure of  $\text{Re}_2\text{Cl}_8^{2-}$  at the CASSCF and CASPT2 Level with the 12/12 Active Space and Different Basis Sets<sup>a</sup>

method	$R_{\text{Re-Re}}$	$R_{\text{Re-Cl}}$	$\angle_{\text{ReReCl}}$
CASSCF B1	2.267	2.398	105.06
CASPT2 B1	2.268	2.397	103.91
CASSCF B2	2.256	2.390	104.87
CASPT2 B2	2.259	2.304	103.44
exptl <sup>1</sup>	$2.241 \pm 0.007$	$2.29 \pm 0.02$	$103.7 \pm 2.1$

<sup>a</sup> Bond distances in angstroms and angles in degrees.

high angular momentum functions (g on Re and f on Cl) is necessary to describe correctly the dynamical correlation effects on the structure. It is also clear that a treatment, which includes dynamic correlation effects, is needed to describe the system already in the ground state. All the excitation energies were thus calculated at the CASPT2/B2 geometry.

The calculations were carried out using the active space formed by 12 active electrons in 12 active orbitals. In Figure 2, we present these active orbitals. They are nicely paired such that the sum of the occupation numbers for the bonding and antibonding orbitals of a given type is almost exactly two. We note that the two bonding Re–Cl orbitals are mainly located on Cl as expected, while the antibonding orbitals have large contributions from  $3d_{x^2-y^2}$ . The occupation is low, and these orbitals are thus almost empty and may be used as acceptor orbitals for electronic transitions.

The strongest bond between the two Re atoms is the  $\sigma$  bond, with an occupation number of  $\eta_b = 1.92$  of the bonding and  $\eta_a = 0.08$  of the antibonding natural orbital. We can estimate the effective bond order as  $(\eta_b - \eta_a)/(\eta_b + \eta_a)$ . For the  $\sigma$  bond we obtain the value 0.92. The corresponding value for the  $\pi$  bond is 1.74 (note that only one component of the  $\pi$  orbitals is shown in the figure). The  $\delta$  pair gives an effective bond order of only 0.54. Adding up these numbers results in a total effective bond order of 3.20 for  $\text{Re}_2\text{Cl}_8^{2-}$ .

**Table 2.** Spin-Free Excitation Energies in  $\text{Re}_2\text{Cl}_8$  (in eV)<sup>a</sup>

state	$\Delta E$ (CAS)	$\Delta E$ (PT2)	exptl <sup>b</sup>	$Q$ (Re)
$\delta \rightarrow \delta^*$ , ${}^1A_{2u}$	3.08	2.03 (0.0037)	1.82 (0.023)	1.03
$\delta \rightarrow \pi^*$ , ${}^1A_{1g}$	2.90	2.29 (f)	2.19 (weak)	1.03
$\pi \rightarrow \delta^*$ , ${}^1E_g$	3.41	2.70 (f)	2.60 ( $\epsilon = 65$ )	1.04
$\delta \rightarrow \pi^*$ , $\pi \rightarrow \delta^*$ , ${}^1E_g$	3.87	3.10 (f)	2.93 (very weak)	1.04
$\delta \rightarrow \sigma^*$ , ${}^1B_{1u}$	4.47	3.10 (f)		1.00
$\delta \rightarrow \delta_{x^2-y^2}$ , ${}^1A_{2g}$	3.96	3.37 (f)		1.11
$(\delta, \pi) \rightarrow (\delta^*)^2$ , ${}^1E_u$	4.20	3.38 ( $0.29 \times 10^{-3}$ )	3.35 ( $\epsilon = \epsilon_1$ ) <sup>c</sup>	1.04
Cl (3p) $\rightarrow \delta^*$ LMCT, ${}^1E_u$	6.37	3.56 ( $0.60 \times 10^{-4}$ )	3.48 ( $\epsilon = \epsilon_2$ ) <sup>c</sup>	0.84
$\delta \rightarrow \delta_{x^2-y^2}$ , ${}^1A_{1u}$	4.24	3.59 (f)		1.13
$\pi \rightarrow \pi^*$ , ${}^1A_{1u}$	5.02	3.76 (f)		1.04
$(\delta, \pi) \rightarrow (\delta^*)^2$ , ${}^1E_u$	4.81	3.80 ( $0.92 \times 10^{-4}$ )		1.04
$(\delta, \pi) \rightarrow (\delta^*\pi^*)$ , ${}^1A_{1g}$	5.01	3.91 (f)		1.05
$\pi \rightarrow \pi^*$ , ${}^1B_{1u}$	5.17	4.00 (f)		1.05
Cl (3p) $\rightarrow \delta^*$ , LMCT, ${}^1E_u$	6.54	4.08 (0.08)	3.83 (intense)	0.88
$\sigma \rightarrow \delta^*$ , $\pi \rightarrow \pi^*$ , ${}^1B_{1u}$	6.01	4.13 (f)		1.05
$\pi \rightarrow \delta_{x^2-y^2}$ , ${}^1E_u$	6.15	4.17 (0.009)		1.08
$(\delta, \pi) \rightarrow (\delta^*\pi^*)$ , ${}^1B_{2g}$	5.66	4.30 (f)		1.04
$\delta\pi \rightarrow \delta^*\sigma^*$ , ${}^1E_u$	6.79	4.40 ( $1.0 \times 10^{-4}$ )	4.42 (complex)	1.03
$\sigma \rightarrow \sigma^*$ , $\pi \rightarrow \pi^*$ , ${}^1A_{2u}$	6.66	4.56 (0.015)	4.86 (intense)	1.04

<sup>a</sup> Oscillator strengths are given within parentheses.  $Q$  (Re) gives the Mulliken charge on one Re atom. <sup>b</sup> From ref 4. <sup>c</sup>  $\epsilon_1 + \epsilon_2 = 400$  (ref 4).

The main reduction of the bond order from 4.0 to 3.2 is due to the weakness of the  $\delta$  bond.

**3.2. The Spin-Free Singlet Excited States.** Vertical excitation energies and oscillator strengths, calculated at the spin-free CASSCF and CASPT2 levels, with the 12/12 active space, are reported in Table 2 for singlet states up to 4.56 eV above the ground state, together with the experimental band maxima and intensities reported by Trogler et al.<sup>4</sup>

The lowest band detected experimentally peaks at 1.82 eV ( $14700 \text{ cm}^{-1}$ ) with an oscillator strength of 0.023. It has been assigned to the  $\delta \rightarrow \delta^*$  ( ${}^1A_{1g} \rightarrow {}^1A_{2u}$ ) transition. Our 12/12 calculation predicts an excitation energy of 2.03 eV at the CASPT2 level with an oscillator strength equal to 0.004. The various 16/14 calculations predict a CASPT2 excitation energy that varies between 1.68 and 1.74 eV. The

oscillator strength varies between 0.007 and 0.092, which shows that this quantity is sensitive to the active space. The low energy of this transition is of course a result of the weak  $\delta$  bond, which places the  $\delta^*$  orbital at low energy. The earlier CASSCF study by Blaudeau et al.<sup>5</sup> gave the energy 3.20 eV.

In the region of weak absorption between 1.98 and 3.10 eV (16000–25000  $\text{cm}^{-1}$ ), the first weak peak occurs at 2.19 eV (17675  $\text{cm}^{-1}$ ) and has been assigned to a  $\delta \rightarrow \pi^*$  ( ${}^1A_{1g} \rightarrow {}^2A_{1g}$ ) transition mostly located on Re with little ligand character. We predict it at 2.29 eV, and it is a forbidden transition.

The second weak peak occurs at 2.60 eV (20940  $\text{cm}^{-1}$ ), with  $\epsilon = 65$ . Only perpendicularly polarized progressions of ca. 400  $\text{cm}^{-1}$  are built on this system. The high frequency is thus not attributable to an  $a_{1g}(\text{ReRe})$  mode but was assigned to an excited state  $a_{1g}(\text{ReCl})$  stretch mode (the ground-state frequency is 357  $\text{cm}^{-1}$ ). The transition was tentatively assigned to  ${}^1A_{1g} \rightarrow {}^1A_{1u}$  ( $\delta \rightarrow \delta^*_{x^2-y^2}$ ). Our result does not agree with this assignment. The  $\delta \rightarrow \delta^*_{x^2-y^2}$  transition is predicted at 3.59 eV. We thus prefer to assign the peak at 2.60 eV to a  $\pi \rightarrow \delta^*$  ( ${}^1A_{1g} \rightarrow {}^1E_g$ ) transition, calculated at 2.70 eV.

A weak progression was seen at 2.93 eV (23650  $\text{cm}^{-1}$ ) and was assigned to a  $\pi \rightarrow \delta^*$  ( ${}^1A_{1g} \rightarrow {}^1E_g$ ) transition, calculated at 3.10 eV. We agree with this assignment even if the computed state is a mixture of different excitations. An alternative assignment could be to a  $\delta \rightarrow \sigma^*$  ( ${}^1A_{1g} \rightarrow {}^1B_{1u}$ ) transition.

A series of excited states were found in the region 3.37–3.80 eV above the ground state. A  $\delta \rightarrow \delta^*_{x^2-y^2}$  ( ${}^1A_{1g} \rightarrow {}^1A_{2g}$ ) transition is predicted at 3.37 eV, but we do not assign it to any of the observed bands. A band measured at 3.35 eV is assigned to the double excitation  $(\delta, \pi) \rightarrow (\delta^*)^2$  ( ${}^1A_{1g} \rightarrow {}^1E_u$ ). Trogler et al., on the other hand, assigned it to a LMCT transition (see in a following discussion). The computed energy is 3.38 eV (3.07–3.11 eV with the 16/14 active space) with an oscillator strength equal to 0.0003.

The computed  $\delta \rightarrow \delta^*_{x^2-y^2}$  ( ${}^1A_{1g} \rightarrow {}^1A_{1u}$ ) transition at 3.59 eV, the  $\pi \rightarrow \pi^*$  ( ${}^1A_{1g} \rightarrow {}^1A_{1u}$ ) transition at 3.76 eV, and the  $(\delta, \pi) \rightarrow (\delta^*)^2$  ( ${}^1A_{1g} \rightarrow {}^1E_u$ ) transition at 3.80 eV (3.45–3.48 eV with the 16/14 active space) do not correspond to any of the observed features in the spectrum.

Two bands with a total  $\epsilon$  of 400 have been assigned to charge transfer, CT, states. They occur at 3.35 and 3.48 eV, respectively. It was suggested that they correspond to two  $A_{2u}$  spin-orbit components of two close-lying  ${}^3E_u$  states.<sup>3</sup> We have not studied the triplet LMCT states, but our first singlet CT state was predicted at 3.56 eV, corresponding to a  $\text{Cl}(3p) \rightarrow \delta^*$  ( ${}^1A_{1g} \rightarrow {}^1E_u$ ) LMCT transition. Thus, it seems natural to assign the upper of the two bands to this transition. The peak at 3.35 eV has been assigned to a metal localized transition.

A  $(\delta, \pi) \rightarrow (\delta^*, \pi^*)$  ( ${}^1A_{1g} \rightarrow {}^1A_{1g}$ ) transition is predicted at 3.91 eV, and a  $\pi \rightarrow \pi^*$  ( ${}^1A_{1g} \rightarrow {}^1B_{1u}$ ) transition at 4.00 eV. No corresponding experimental bands could be found. An intense CT state is found in the experimental spectrum at 3.83 eV, and it is assigned to the  $\text{Cl}(3p) \rightarrow \delta^*$  ( ${}^1A_{1g} \rightarrow$

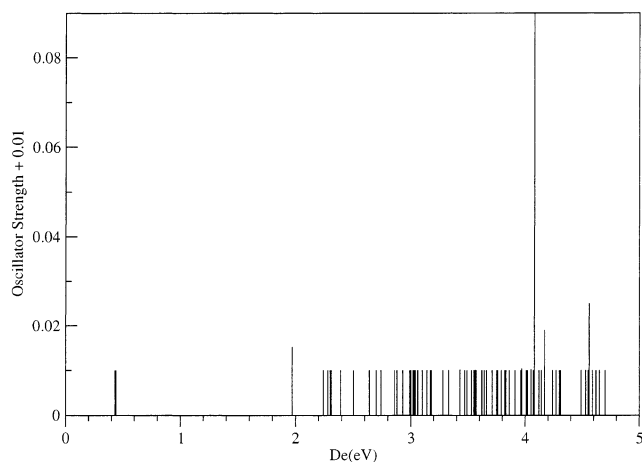


Figure 3. Spin-orbit electronic spectrum of  $\text{Re}_2\text{Cl}_8^{2-}$ .

${}^1E_u$ ) transition that we predict at 4.08 eV with an oscillator strength of 0.08.

Trogler et al. have suggested that the complex band found at 4.42 eV should be a mixture of two LMCT transitions. We find no evidence of this in the calculations, but a weak  ${}^1E_u$  state is found at 4.40 eV and there are other forbidden transitions nearby.

A rather intense band is found at 4.86 eV with a tentative assignment  $\pi \rightarrow \pi^*$  ( ${}^1A_{1g} \rightarrow {}^1A_{2u}$ ). We agree with this assignment and compute the state to occur at 4.56 eV with an oscillator strength of 0.015.

**3.3. The Electronic Spectrum Including Spin–Orbit Splitting.** In order to compute the SO coupling, an SO Hamiltonian matrix was constructed in the basis of all 12/12 CASSCF wave functions corresponding to singlet and triplet states in the region below 5 eV above the ground state. This gives a total of 19 singlet and 26 triplets states, which with spin-orbit interaction result in 97 spin-orbit states. Dynamic correlation energy was introduced by shifting the diagonal of the SO Hamiltonian matrix to the CASPT2 energies.

The spin-orbit electronic spectrum is reported in Figure 3. The oscillator strength is plotted as a function of the energy for all states. In order to show how dense the spectrum is, the states with zero oscillator strength are also reported. This has been done by adding 0.01 to all the oscillator strengths.

The most important of the excited SO states are reported in Table 3. We have in this table for space reasons only included the allowed states ( $A_{2u}$  or  $E_u$ ). The state number in the list of the 97 components is given to indicate where in the spectrum these states occur. We notice that most of the states are triplets, which obtain some intensity through the interaction with nearby singlet states.

The first excited triplet state,  $\delta \rightarrow \delta^*$  ( ${}^1A_{1g} \rightarrow {}^3A_{2u}$ ), is found at 0.37 eV in the spin-free calculation. After spin-orbit coupling is introduced, we find the two components at 0.43 and 0.44 eV, respectively (3447 and 3571  $\text{cm}^{-1}$ ). The computed spin-orbit splitting is thus 124  $\text{cm}^{-1}$ . The upper state is the allowed  $E_u$  component and has now a computed intensity of  $1.1 \times 10^{-6}$ . Blaudeau et al.<sup>5</sup> have found the lowest triplet at 0.44 eV at the CASSCF level, thus

**Table 3.** CASPT2 Excitation Energies in  $\text{Re}_2\text{Cl}_8$  (in eV) Including Spin–Orbit Coupling<sup>a</sup>

state <sup>b</sup>	energy <sup>c</sup>	energy <sup>c</sup>	oscillator strength
2 (T)	0.43 (0.37)	3447	$0.4791 \times 10^{-25}$
3, 4 (T)	0.44 (0.37)	3571	$0.1112 \times 10^{-5}$
5 (S)	1.97 (2.03)	15886	$0.5214 \times 10^{-2}$
13, 14 (T)	2.50 (2.47)	20158	$0.1019 \times 10^{-4}$
28, 29 (T)	3.02 (2.91)	24323	$0.3759 \times 10^{-6}$
31, 32 (T)	3.04 (2.86)	24488	$0.2077 \times 10^{-4}$
36 (T)	3.14 (2.91)	25320	$0.2088 \times 10^{-5}$
39, 40 (T)	3.18 (2.86)	25631	$0.6081 \times 10^{-5}$
42, 43 (T)	3.28 (3.15)	26427	$0.3444 \times 10^{-4}$
45, 46 (S)	3.43 (3.38)	27636	$0.1578 \times 10^{-3}$
51 (T)	3.55 (3.37)	28602	$0.3092 \times 10^{-4}$
58, 59 (T)	3.71 (3.37)	29922	$0.2045 \times 10^{-4}$
64 (T)	3.82 (3.63)	30820	$0.3458 \times 10^{-5}$
67, 68 (T)	3.91 (3.68)	31570	$0.1537 \times 10^{-4}$
72 (T)	3.97 (3.68)	32006	$0.3958 \times 10^{-3}$
73, 74 (T)	4.01 (3.63)	32308	$0.2976 \times 10^{-4}$
77, 78 (S)	4.05 (3.80)	32673	$0.2070 \times 10^{-3}$
89, 90 (T)	4.53 (4.34)	36534	$0.5822 \times 10^{-4}$
94, 95 (T)	4.62 (4.36)	37262	$0.6757 \times 10^{-5}$
96 (T)	4.65 (4.36)	37501	$0.3803 \times 10^{-4}$

<sup>a</sup> Only the most significant states with nonzero intensity are included. Energies are given in eV and  $\text{cm}^{-1}$ . No LMCT states in this table. <sup>b</sup> The state number is given (1–97) together with the main character of the state, singlet (S) or triplet (T). <sup>c</sup> The first column gives the SO energy (within parentheses the spin-free energy) in eV, the second column in  $\text{cm}^{-1}$ .

confirming the present result. As far as we know, there is no experimental determination of the lowest excited state in the electronic spectrum.

No more triplet states occur below the first singlet state, which is shifted from 2.03 to 1.97 eV when spin–orbit coupling is introduced. The oscillator strength has increased to 0.005. Next, we follow six weakly allowed triplet states in the energy region between 2.47 and 3.15 eV. The oscillator strength varies between  $10^{-5}$  and  $10^{-6}$ . Experimentally, three bands were found in this region, which already have been assigned to  $g \rightarrow g$  transitions with vibrationally induced intensities. We still believe these assignments to be more plausible than assignments to triplet states. It may be noted that the weak  $\delta \rightarrow \pi^*$  ( $A_{1g}$ ) state now occurs at 2.24 eV (2.29 eV at the spin-free level). The  $E_u$  state, which in the spin-free calculation corresponds to an excitation energy of 3.38 eV, is now shifted to 3.43 eV, and the intensity has decreased to almost half its value. In general, spin–orbit coupling introduces energy shifts of the excited states, in addition to the splitting of the triplet states into two components. The shifts can be as large as 0.3 eV in some cases.

However, the introduction of spin–orbit coupling does not in general change any of the qualitative features of the spectrum. There is a small shift in the energies and intensities, but we do not see any new states with intensities appreciably different from zero. We may, however, have lost some information because we have not studied the LMCT triplet states and the corresponding effects of spin–orbit splitting.

#### 4. Conclusions

We have presented the results of the CASSCF/CASPT2 study of  $\text{Re}_2\text{Cl}_8^{2-}$ . The ground state geometry has been optimized, and the electronic spectrum has been calculated. From the bond order analysis, we conclude that the Re–Re bond has an effective bond order of 3.2. The reason is mainly the large occupation of the antibonding  $\delta^*$  orbital. Whether it should be called a triple or a quadruple bond is a matter of definition. Nobody would argue that there is a bond between two hydrogen atoms at a distance of 10 Å from each other. An HF calculation would, however, give one doubly occupied “bonding” orbital. A CASSCF calculation with two active orbitals would on the other hand give two orbitals, one bonding and one antibonding, both with the occupation number one, leading to a net bond order of zero. The  $\delta$  bond in  $\text{Re}_2\text{Cl}_8^{2-}$  is between these with a net bond order of about 0.5. Whether this should be called weak bond or half a bond is a matter of nomenclature. The alternatives are to describe the bonding as a “weak” quadruple bond or as a bond involving four electron pairs with an effective bond order of about three. The latter description is more precise.

The calculation of the electronic spectrum has made it possible to assign all experimental features and in no case does the computed transition energy differ more than 0.3 eV from the measured band maximum. We consider this quite satisfactory, considering the many uncertainties that are inherent in a comparison between vertical excitation energies of a gas phase quantum chemical calculation and experimental band maxima obtained from measurements on single crystals.

**Acknowledgment.** This work has been supported by the Italian Ministero dell’Istruzione dell’Università e della Ricerca and the Swedish Research council.

IC0261068